


Standard model prediction for cosmological 21 cm circular polarization

Lingyuan Ji^{*} and Marc Kamionkowski[†]

*Department of Physics and Astronomy, Johns Hopkins University,
3400 North Charles Street, Baltimore, Maryland 21218, USA*

Keisuke Inomata[‡]

*Research Center for the Early Universe (RESCEU), Graduate School of Science,
The University of Tokyo, Hongo 7-3-1 Bunkyo-ku, Tokyo 113-0033, Japan*

 (Received 25 June 2020; revised 8 October 2020; accepted 9 December 2020; published 7 January 2021)

Before cosmic reionization, hydrogen atoms acquire a spin polarization quadrupole through interaction with the anisotropic 21-cm radiation field. The interaction of this quadrupole with anisotropies in the cosmic microwave background (CMB) radiation field gives a net spin orientation to the hydrogen atoms. The 21-cm radiation emitted by these spin-oriented hydrogen atoms is circularly polarized. Here, we reformulate succinctly the derivation of the expression for this circular polarization in terms of Cartesian (rather than spherical) tensors. We then compute the angular power spectrum of the observed Stokes- V parameter in the standard Λ CDM cosmological model and show how it depends on redshift, or equivalently, the observed frequency.

DOI: [10.1103/PhysRevD.103.023516](https://doi.org/10.1103/PhysRevD.103.023516)

The redshifted 21-cm line of neutral hydrogen provides the most promising probe of the cosmological “dark ages,” the epoch after CMB photons are emitted and before the first stars are formed. While the majority of theoretical work has focused on intensity fluctuations of the 21-cm radiation [1–5], there has also been some work on the linear polarization [6,7].

The *circular* polarization of the redshifted 21-cm line was considered in Refs. [8,9]. Reference [8] showed that circular polarization arises from an interaction between CMB anisotropies and the atom’s spin polarization induced by anisotropies in the 21-cm radiation incident on the atom. Reference [9] then focused on the circular polarization from the CMB quadrupole induced by primordial gravitational waves and discussed the prospects to detect an inflationary gravitational-wave background in this way.

In this paper, we translate the central atomic-physics results of Ref. [8], which were presented in terms of spherical tensors, in terms of more intuitive Cartesian tensors. We then calculate the angular power spectrum for the 21-cm polarization that arises at second order in the primordial-density-perturbation amplitude in the standard Λ CDM cosmological model. We employ aspects of the total-angular-momentum (TAM) formalism [10,11] to derive the results in a relatively economical fashion. We then evaluate the circular-polarization angular power spectrum numerically and determine its

dependence on the observed frequency, or equivalently, the redshift of the emitter. Throughout this paper we use units in which $c = \hbar = 1$.

The signal calculated here provides a *guaranteed* target that must be detected and observed before the circular polarization can be used to probe inflationary gravitational waves. Detection of this signal can also constrain some of the uncertain 21-cm physics, complementing constraints from the intensity and linear polarization. Furthermore, this signal will also probe the CMB quadrupole at redshifts higher than those proposed in Ref. [12], and so further reduce the cosmic variance by accessing even more surfaces of last scattering.

Consider the circular polarization $V(\chi, \hat{n})$ of the 21-cm radiation that arrives to us from a comoving distance χ and direction \hat{n} . The hydrogen atoms at the point $\vec{x} = \chi\hat{n}$ are immersed in a 21-cm radiation field that has anisotropies arising from local gas-density inhomogeneities. This then induces a spin-polarization tensor with a quadrupole aligned with the quadrupole of the 21-cm radiation. The atoms are also immersed in a CMB radiation field that also has anisotropies, which are mainly determined by the density fluctuations on the last scattering surface. Reference [8] shows that a net spin orientation of the neutral hydrogen arises from the misalignment of the atomic spin-polarization quadrupole and the CMB quadrupole, which leads to spontaneous and stimulated emission of 21 cm radiation in direction $-\hat{n}$ that is circularly polarized. The spin quadrupole moment of the hydrogen atoms at comoving position \vec{x} (at the conformal time

^{*}lingyuan.ji@jhu.edu

[†]kamion@jhu.edu

[‡]inomata@resceu.s.u-tokyo.ac.jp

$\eta = \eta_0 - \chi$, where η_0 is the conformal time today) can be represented as a rank-2 tensor $\gamma_{ab}(\vec{x}, \eta)$ that is symmetric ($\gamma_{ab} = \gamma_{ba}$) and trace-free ($\gamma_{bb} = 0$)—it is given explicitly in Eq. (3) of Ref. [8]. Likewise, the CMB temperature quadrupole at that point is $t_{ab}(\vec{x}, \eta) \equiv \int d^2\hat{u} (3\hat{u}_a\hat{u}_b - \delta_{ab})\Theta(\vec{x}, \hat{u}, \eta)$, where $\Theta(\vec{x}, \hat{u}, \eta) \equiv T(\vec{x}, \hat{u}, \eta)/T_\gamma(\eta) - 1$ with $T(\vec{x}, \hat{u}, \eta)$ the CMB temperature at (\vec{x}, η) arriving from direction \hat{u} and $T_\gamma(\eta)$ the mean CMB temperature at η .

The circular polarization is parity-odd and is thus a pseudoscalar. We therefore infer that the circular polarization must be

$$V(\chi, \hat{n}) = C(\eta_0 - \chi)\epsilon_{abc}n_a\gamma_{bd}(\chi\hat{n}, \eta_0 - \chi)t_{cd}(\chi\hat{n}, \eta_0 - \chi), \quad (1)$$

as this is the only pseudoscalar that can be constructed from n_a , γ_{ab} , and t_{ab} , and the Levi-Civita symbol ϵ_{abc} . The coefficient C can be determined by comparing Eq. (1), Eqs. (4) and (46) in Ref. [8], and the translation [e.g., Eq. (3) in that paper] between spherical and Cartesian tensors. The result is

$$C(\eta) \equiv \sqrt{\frac{2}{3\pi}} \frac{(1+z)T_s(\eta)K_{\text{mag}}\tau(\eta)}{A[1+0.75\tilde{x}_\alpha(\eta)]}, \quad (2)$$

where $K_{\text{mag}} = 1.65 \times 10^{-12} \text{ s}^{-1}$; $A = 2.86 \times 10^{-15} \text{ s}^{-1}$ is the Einstein coefficient of the hyperfine transition; z the redshift at conformal time η ; $T_s(\eta)$ the spin temperature at that time; and $\tilde{x}_\alpha(\eta)$ the coefficient describing the rate of dealignment of polarized hydrogen atoms. Here, $\tau(\eta)$ is the optical depth in the 21-cm line.

The next step is to determine the connection between the spin-polarization tensor $\gamma_{ab}(\vec{x}, \eta)$ and the linear-theory fractional density perturbation $\delta(\vec{x}, \eta)$ at that time. This tensor can again be written in terms of spherical tensors, and the spherical-tensor components induced by one Fourier mode $\tilde{\delta}(\vec{k}, \eta)$, of wave vector \vec{k} , of the density field are [Eq. (4) in Ref. [8]],

$$\tilde{\mathcal{P}}_{2m}(\vec{k}, \eta) = \sqrt{\frac{4\pi}{5}} D(\eta) \tilde{\delta}(\vec{k}, \eta) Y_{2m}(\hat{k}), \quad (3)$$

where Y_{lm} are the spherical harmonics. Here,

$$D(\eta) \equiv \frac{1}{20\sqrt{2}} \frac{T_*}{T_\gamma(\eta)} \left[1 - \frac{T_\gamma(\eta)}{T_s(\eta)} \right] \frac{f\tau(\eta)}{1 + \tilde{x}_\alpha(\eta) + \tilde{x}_c(\eta)}, \quad (4)$$

is a \vec{k} -independent quantity, where $T_* = 68 \text{ mK}$ is the hyperfine splitting in temperature unit, f is the growth rate of structure (which is unity during the matter domination), and $\tilde{x}_c(\eta)$ describes the rate of collisions with other hydrogen atoms. In terms of Cartesian tensors, the relation must take the form,

$$\gamma_{ab}(\vec{x}, \eta) = F(\nabla^2) \left(\nabla_a \nabla_b - \frac{1}{3} \delta_{ab} \nabla^2 \right) \delta(\vec{x}, \eta), \quad (5)$$

(where $\nabla_a \equiv \partial/\partial x_a$) given that any symmetric trace-free rank-2 tensor constructed from the scalar $\delta(\vec{x})$ must be proportional to $[\nabla_a \nabla_b - (\delta_{ab}/3)\nabla^2]\delta(\vec{x})$. In Fourier space, this relation becomes

$$\tilde{\gamma}_{ab}(\vec{k}, \eta) = -F(-k^2) \left(k_a k_b - \frac{k^2}{3} \delta_{ab} \right) \tilde{\delta}(\vec{k}, \eta). \quad (6)$$

The function $F(x)$ can be determined, for example, by taking $\vec{k} = k\hat{z}$ (which makes γ_{ab} diagonal) and comparing Eq. (6) with Eq. (3). Doing so, we find $F(-k^2) = -D/(\sqrt{2}k^2)$, or

$$\tilde{\gamma}_{ab}(\vec{k}, \eta) = \frac{D(\eta)}{\sqrt{2}} \left(\hat{k}_a \hat{k}_b - \frac{\delta_{ab}}{3} \right) \tilde{\delta}(\vec{k}, \eta). \quad (7)$$

We now review the relation between the CMB-anisotropy tensor $t_{ab}(\vec{x}, \eta)$ and $\delta(\vec{x}, \eta)$. Since $t_{ab}(\vec{x}, \eta)$ is the quadrupole moment of the CMB anisotropy observed at (\vec{x}, η) during the matter-dominated era, we can obtain it from the Sachs-Wolfe effect. Thus,

$$\begin{aligned} t_{ab}(\vec{x}, \eta) &= \int d^2\hat{u} (3\hat{u}_a\hat{u}_b - \delta_{ab})\Theta(\vec{x}, \hat{u}, \eta) \\ &= - \int d^2\hat{u} \left(\hat{u}_a\hat{u}_b - \frac{\delta_{ab}}{3} \right) \Phi[\vec{x} + \hat{u}(\eta - \eta_{\text{ls}}), \eta_{\text{ls}}], \end{aligned} \quad (8)$$

where $\Phi(\vec{x}, \eta_{\text{ls}})$ is the Newtonian-gauge gravitational potential [13] at the conformal time η_{ls} of the CMB surface of last scatter. Using the shift formula, this relation can be written in Fourier space as

$$\tilde{t}_{ab}(\vec{k}, \eta) = - \left[\int d^2\hat{u} \left(\hat{u}_a\hat{u}_b - \frac{\delta_{ab}}{3} \right) e^{i\vec{k}\cdot\hat{u}(\eta - \eta_{\text{ls}})} \right] \tilde{\Phi}(\vec{k}, \eta_{\text{ls}}). \quad (9)$$

The integral over \hat{u} can be evaluated by using the plane-wave expansion and taking $\vec{k} = k\hat{z}$. The gravitational-potential perturbation can be related to the density perturbation through the (Fourier-space) Poisson equation, $(k/a)^2 \tilde{\Phi}(\vec{k}, \eta) = 4\pi G \bar{\rho} \tilde{\delta}(\vec{k}, \eta)$, with a the scale factor and $\bar{\rho} = 3H_0^2 \Omega_m / (8\pi G a^3)$ the mean density in the matter dominated era. Finally, we arrive at

$$\tilde{t}_{ab}(\vec{k}, \eta) = \frac{6\pi H_0^2 \Omega_m}{a(\eta_{\text{ls}})k^2} j_2[k(\eta - \eta_{\text{ls}})] \left(\hat{k}_a \hat{k}_b - \frac{\delta_{ab}}{3} \right) \tilde{\delta}(\vec{k}, \eta_{\text{ls}}), \quad (10)$$

where $j_J(x)$ are the spherical Bessel functions.

Next, we relate the matter perturbation $\delta(\vec{x}, \eta)$ at conformal time $\eta = \eta_0 - \chi$ and η_{ls} to the primordial curvature perturbation $\mathcal{R}(\vec{x})$ generated during inflation. Since both times are within the matter dominated era, the relation in Fourier space takes the form [13]

$$\tilde{\delta}(\vec{k}, \eta) = \frac{2k^2}{5H_0^2 \Omega_m} T(k) D_+(\eta) \tilde{\mathcal{R}}(\vec{k}). \quad (11)$$

Here $D_+(\eta)$ is the linear structure growth function and $T(k)$ is the matter transfer function normalized to unity at large scales.

We now expand the primordial curvature perturbation

$$\mathcal{R}(\vec{x}) = \sum_{kJM} \mathcal{R}_{kJM} [4\pi i^J \Psi_{(JM)}^k(\vec{x})], \quad (12)$$

in terms of scalar TAM waves $\Psi_{(JM)}^k(\vec{x}) \equiv j_J(kx) Y_{JM}(\hat{x})$. Here \sum_k is a shorthand for $\int k^2 dk / (2\pi)^3$. We assume that $\mathcal{R}(\vec{x})$ is a statistically homogeneous and isotropic random field in which case,

$$\langle (\mathcal{R}_{kJM})^* \mathcal{R}_{k'J'M'} \rangle = \delta_{kk'} \delta_{JJ'} \delta_{MM'} P_{\mathcal{R}}(k), \quad (13)$$

where the angle brackets denote an average over all realizations of the random field. Here $\delta_{kk'}$ is a shorthand for $(2\pi)^3 \delta_D(k - k') / k^2$, and $P_{\mathcal{R}}(k)$ is the primordial curvature power spectrum.

Likewise, a symmetric trace-free tensor field $h_{ab}(\vec{x})$ can be expanded in much the same manner

$$h_{ab}(\vec{x}) = \sum_{\alpha} \sum_{kJM} h_{kJM}^{\alpha} [4\pi i^J \Psi_{(JM)ab}^{k,\alpha}(\vec{x})], \quad (14)$$

where the sum on α is over the five types ($\alpha = \text{L, VE, VB, TE, TB}$) of tensor TAM waves. Given that we are here concerned only with primordial density perturbations, we will require only the longitudinal (L) mode which can be obtained from the scalar TAM wave from

$$\Psi_{(JM)ab}^{k,\text{L}}(\vec{x}) = \frac{1}{k^2} \sqrt{\frac{3}{2}} \left(\nabla_a \nabla_b - \frac{1}{3} \delta_{ab} \nabla^2 \right) \Psi_{(JM)}^k(\vec{x}). \quad (15)$$

These tensor TAM waves can be written in terms of radial functions $R_J^{\text{L}\beta}(kx)$ and tensor spherical harmonics $Y_{(JM)ab}^{\beta}(\hat{x})$ as,

$$\Psi_{(JM)ab}^{k,\text{L}}(\vec{x}) = \sum_{\beta} R_J^{\text{L}\beta}(kx) Y_{(JM)ab}^{\beta}(\hat{x}). \quad (16)$$

Here, the sum on β is over $\beta = \{\text{L, VE, TE}\}$, the radial eigenfunctions can be inferred from Eq. (94) in Ref. [10], and the tensor spherical harmonics are defined in Eq. (91) in that paper.

Thus, we can write

$$\gamma_{ab}(\vec{x}, \eta) = \sum_{kJM} T_{\gamma}(k, \eta) \mathcal{R}_{kJM} [4\pi i^J \Psi_{(JM)ab}^{k,\text{L}}(\vec{x})], \quad (17)$$

and similarly for t_{ab} in terms of a temperature transfer function $T_t(k, \eta)$. The transfer functions $T_{\gamma}(k, \eta)$ and $T_t(k, \eta)$ can be determined by combining Eqs. (7) and (10) with Eq. (11), then using Eqs. (8) and (104) of Ref. [10] to convert the Fourier amplitudes to TAM coefficients. Doing so, we find

$$T_{\gamma}(k, \eta) = -\frac{2k^2 D(\eta)}{5\sqrt{3} H_0^2 \Omega_m} T(k) D_+(\eta), \quad (18)$$

$$T_t(k, \eta) = -\frac{12\sqrt{2}\pi}{5\sqrt{3}} j_2[k(\eta - \eta_{\text{ls}})] T(k) \frac{D_+(\eta_{\text{ls}})}{a(\eta_{\text{ls}})}. \quad (19)$$

In 21-cm measurements, the light received in a given frequency band corresponds to light emitted over a corresponding range of redshifts or, equivalently, comoving distances. Here we surmise that the circular polarization is measured in a frequency interval that corresponds to emission from a shell of comoving-distance width $\Delta\chi$ centered at χ . The observed circular polarization in direction \hat{n} will then be

$$\begin{aligned} V_{\chi}(\hat{n}) &\equiv \int_{\chi - \Delta\chi/2}^{\chi + \Delta\chi/2} \frac{d\chi'}{\Delta\chi} V(\chi', \hat{n}) \\ &\simeq C(\eta_0 - \chi) \epsilon_{abc} n_a \gamma_{bd}(\chi \hat{n}, \eta_0 - \chi) t_{cd}(\chi \hat{n}, \eta_0 - \chi). \end{aligned} \quad (20)$$

The approximation in the second equality will hold as long as the redshift evolution of t_{ab} , γ_{ab} and C is relatively slow over the integration interval. This approximation is valid when discussing circular polarization on angular scales θ larger than $\Delta\chi/\chi$ (or multipole moments $l \lesssim \chi/\Delta\chi$), as perturbations contributing to these angular scales (those with comoving wave number $k < 1/\Delta\chi$) will be slowly varying in the integral in Eq. (20).

Inserting Eq. (17) and the similar one for t_{ab} into Eq. (20), the spherical-harmonic expansion coefficients $V_{\chi(lm)} \equiv \int d^2 \hat{n} Y_{lm}^*(\hat{n}) V_{\chi}(\hat{n})$ then evaluate to

$$\begin{aligned}
 V_{\chi(lm)} = & C(\eta_0 - \chi) \sum_{(kJM)_\gamma} \sum_{(kJM)_i} \mathcal{R}_{(kJM)_\gamma} \mathcal{R}_{(kJM)_i} T_\gamma(k_\gamma, \eta_0 - \chi) T_i(k_i, \eta_0 - \chi) \\
 & \times [\tilde{R}_{J_\gamma}^{\text{VE}}(k_\gamma \chi) \tilde{R}_{J_i}^{\text{VE}}(k_i \chi) K_{lm(JM)_\gamma(JM)_i}^{\text{VB,VE}} + \tilde{R}_{J_\gamma}^{\text{TE}}(k_\gamma \chi) \tilde{R}_{J_i}^{\text{TE}}(k_i \chi) K_{lm(JM)_\gamma(JM)_i}^{\text{TB,TE}}], \quad (21)
 \end{aligned}$$

where $\tilde{R}_J^\beta(x) \equiv 4\pi i^J R_J^{L\beta}(x)$. Here, $K_{lm(JM)_\gamma(JM)_i}^{\text{VB,VE}}$ and $K_{lm(JM)_\gamma(JM)_i}^{\text{TB,TE}}$ involve Wigner-3j symbols and can be inferred from the integrals in Eqs. (64) and (66), respectively, of Ref. [11]; they are nonzero only for $l + J_\gamma + J_i = \text{odd}$. Using Wick's theorem and Eq. (13) for the primordial power spectrum, plus the summation properties of the K -factors, the angular circular-polarization power spectrum $C_l^{V_\chi V_\chi} \equiv \langle |V_{\chi(lm)}|^2 \rangle$ is found to be

$$\begin{aligned}
 C_l^{V_\chi V_\chi} = & |C(\eta_0 - \chi)|^2 \sum_{J_\gamma, J_i(\text{odd})} \sum_{k_\gamma, k_i} P_{\mathcal{R}}(k_\gamma) P_{\mathcal{R}}(k_i) \{T_\gamma(k_\gamma) T_i(k_i) [T_\gamma(k_\gamma) T_i(k_i) - T_\gamma(k_i) T_i(k_\gamma)]\}_{\eta=\eta_0-\chi} \\
 & \times \frac{(2J_\gamma + 1)(2J_i + 1)}{4\pi} \left| \tilde{R}_{J_\gamma}^{\text{VE}}(k_\gamma \chi) \tilde{R}_{J_i}^{\text{VE}}(k_i \chi) \begin{pmatrix} l & J_\gamma & J_i \\ 0 & +1 & -1 \end{pmatrix} - \tilde{R}_{J_\gamma}^{\text{TE}}(k_\gamma \chi) \tilde{R}_{J_i}^{\text{TE}}(k_i \chi) \begin{pmatrix} l & J_\gamma & J_i \\ 0 & +2 & -2 \end{pmatrix} \right|^2. \quad (22)
 \end{aligned}$$

Here “ $J_\gamma J_i(\text{odd})$ ” means the sum of all terms where $J_\gamma + J_i + l$ is an odd number for a given l , and the combination of transfer functions in the curly brackets should be evaluated at $\eta = \eta_0 - \chi$. The all-sky mean-square signal is $\overline{V_\chi^2} \equiv \int d^2 \hat{n} |V_\chi(\hat{n})|^2 / (4\pi)$. By Parseval's theorem, it has the expectation value $\langle \overline{V_\chi^2} \rangle = \sum_l (2l + 1) C_l^{V_\chi V_\chi} / (4\pi)$.

Evaluations of the angular power spectrum Eq. (22) for the circular polarizations emitted at three redshifts $z = 17, 24, 80$ [redshifted frequencies $\nu_{\text{obs}} = 1420/(1 + z)$ MHz] are shown in Fig. 1. The three redshifts correspond roughly to the times when X-rays from stellar remnants starts to heat the gas ($z \sim 17$), when the Lyman- α photons from the first stars start to heat the hydrogen atoms ($z \sim 24$), and when the spin temperature begins to approach the CMB temperature ($z \sim 80$). The functions $C(\eta)$ and $D(\eta)$ depend on the details of the ionization history and heating of the

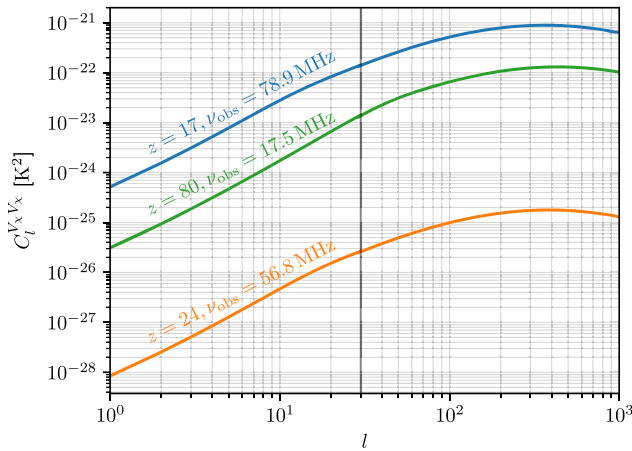


FIG. 1. Angular power spectra $C_l^{V_\chi V_\chi}$ of the 21-cm circular polarization sourced by scalar perturbation at redshifts $z = 17, 24, \text{ and } 80$, corresponding to the redshifted frequencies $\nu_{\text{obs}} = 1420/(1 + z)$ MHz = 78.9 MHz, 56.8 MHz, 17.5 MHz. The signals peak around $l \sim 400$, corresponding to an angular scale $\theta \sim 180^\circ/l \sim 0.5^\circ$.

IGM and are quite uncertain, particularly at the lower redshifts ($z \lesssim 20$) associated with the epoch of reionization. To illustrate, we use here the model detailed in Appendix B of Ref. [14], with one modification $A_\alpha \rightarrow 8$ so that $T_{21} \sim -100$ mK at $z = 17$. For low multipoles ($l \leq 30$), Eq. (22) is evaluated exactly using WIGXJPF [15] to evaluate the Wigner-3j symbols. For high multipoles ($l > 30$), we use the flat-sky approximation [16,17]. Also, we have numerically confirmed that the angular power spectrum is dominated by the autocorrelation term in the Wick expansion [i.e., the first term in the square brackets in Eq. (22)].

The numerical results indicate that the angular power spectra at different redshifts differ primarily in their magnitude, while the angular (l) dependence is similar (though not exactly). The power is spread over a wide range of angular scales but peaks at $l \sim 400$ corresponding to an

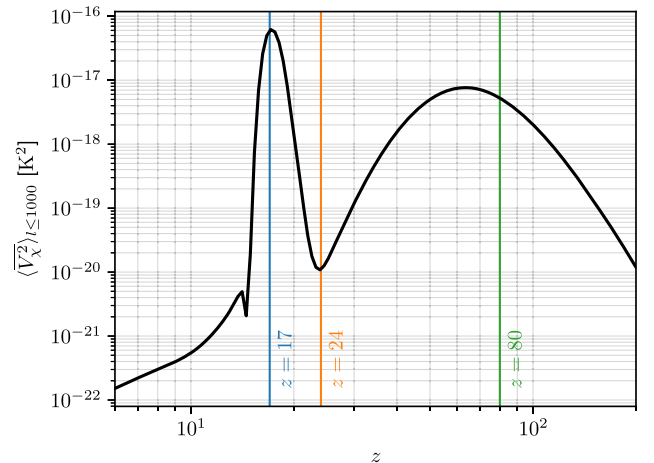


FIG. 2. The mean-square signal $\langle \overline{V_\chi^2} \rangle_{l \leq 1000} \equiv \sum_{l=0}^{1000} (2l + 1) C_l^{V_\chi V_\chi} / (4\pi)$ as a function of the redshift. The three vertical lines correspond the power spectra plotted in Fig. 1. The strongest signal is sourced around $z = 17$, corresponding to a redshifted frequency $\nu_{\text{obs}} = 78.9$ MHz.

angular scale $\sim 0.5^\circ$. This is roughly the angular scale corresponding to the transition scale in the matter transfer function $T(k)$ for those redshifts. We indicate the redshift dependence of the signal through the mean-square circular polarization, $\langle V_\chi^2 \rangle_{l \leq 1000} \equiv \sum_{l=0}^{1000} (2l+1) C_l^{V_\chi V_\chi} / (4\pi)$ shown as a function of redshift in Fig. 2. Again, there are considerable uncertainties in this calculation, primarily at lower redshifts, although the gross features should be reliable. We see that the signal strength can vary quite rapidly with frequency at frequencies $\nu \simeq 80$ MHz corresponding to the beginning of the x-ray heating. The detailed frequency dependence here is, however, uncertain. There is a more robust prediction for a second, wider, peak at $\nu \simeq 20$ MHz.

To close, we have evaluated the circular polarization of the 21-cm radiation from the dark ages and epoch of reionization that arises at second order in the primordial-density-perturbation amplitude. We leave a detailed exploration of the detectability of the signal, and strategies for

detection, to future work. Still, the estimates of the signal from the gravitational-wave induced CMB quadrupole [9] suggest that the signal may be within reach of an ambitious lunar radio base [18]; if so, the density-perturbation signal considered here, which is at least $1/r$ ($\gtrsim 14$, r : tensor-to-scalar ratio [19]) times bigger, should also be within reach. The techniques described here can also be generalized to models with primordial gravitational waves or vector perturbations. It will also be interesting in future work to investigate the dependence of the signal on the detailed physics of reionization and to consider cross-correlations of this signal with other observables [20–23].

We thank E. D. Kovetz, J. L. Bernal, and K. Boddy for useful discussions and B. Wang for providing an ionization-history code. L. J. and M. K. were supported by NSF Grant No. 1519353, NASA Grant No. NNX17AK38G, and the Simons Foundation and K. I. was supported by JSPS KAKENHI Grants No. 15H02082 and No. 20H05248.

-
- [1] A. Loeb and M. Zaldarriaga, Measuring the Small—Scale Power Spectrum of Cosmic Density Fluctuations Through 21 cm Tomography Prior to the Epoch of Structure Formation, *Phys. Rev. Lett.* **92**, 211301 (2004).
- [2] S. Furlanetto, S. P. Oh, and F. Briggs, Cosmology at low frequencies: The 21 cm transition and the high-redshift Universe, *Phys. Rep.* **433**, 181 (2006).
- [3] A. Lewis and A. Challinor, The 21 cm angular-power spectrum from the dark ages, *Phys. Rev. D* **76**, 083005 (2007).
- [4] J. R. Pritchard and A. Loeb, 21-cm cosmology, *Rep. Prog. Phys.* **75**, 086901 (2012).
- [5] M. F. Morales and J. S. B. Wyithe, Reionization and cosmology with 21 cm fluctuations, *Annu. Rev. Astron. Astrophys.* **48**, 127 (2010).
- [6] D. Babich and A. Loeb, Polarization of 21 cm radiation from the epoch of reionization, *Astrophys. J.* **635**, 1 (2005).
- [7] S. De and H. Tashiro, Galactic Faraday rotation effect on polarization of 21 cm lines from the epoch of reionization, *Phys. Rev. D* **89**, 123002 (2014).
- [8] C. M. Hirata, A. Mishra, and T. Venumadhav, Detecting primordial gravitational waves with circular polarization of the redshifted 21 cm line. I. Formalism, *Phys. Rev. D* **97**, 103521 (2018).
- [9] A. Mishra and C. M. Hirata, Detecting primordial gravitational waves with circular polarization of the redshifted 21 cm line. II. Forecasts, *Phys. Rev. D* **97**, 103522 (2018).
- [10] L. Dai, M. Kamionkowski, and D. Jeong, Total angular momentum waves for scalar, vector, and tensor fields, *Phys. Rev. D* **86**, 125013 (2012).
- [11] L. Dai, D. Jeong, and M. Kamionkowski, Wigner-Eckart theorem in cosmology: Bispectra for total-angular-momentum waves, *Phys. Rev. D* **87**, 043504 (2013).
- [12] M. Kamionkowski and A. Loeb, Getting around cosmic variance, *Phys. Rev. D* **56**, 4511 (1997).
- [13] S. Dodelson, *Modern Cosmology* (Academic Press, Amsterdam, Netherlands, 2003), p. 440.
- [14] E. D. Kovetz, V. Poulin, V. Gluscevic, K. K. Boddy, R. Barkana, and M. Kamionkowski, Tighter limits on dark matter explanations of the anomalous EDGES 21 cm signal, *Phys. Rev. D* **98**, 103529 (2018).
- [15] H. T. Johansson and C. Forssn, Fast and accurate evaluation of Wigner 3j, 6j, and 9j symbols using prime factorisation and multi-word integer arithmetic, *SIAM J. Sci. Stat. Comput.* **38**, A376 (2016).
- [16] K. Inomata and M. Kamionkowski, Circular polarization of the cosmic microwave background from vector and tensor perturbations, *Phys. Rev. D* **99**, 043501 (2019).
- [17] W. Hu, Weak lensing of the CMB: A harmonic approach, *Phys. Rev. D* **62**, 043007 (2000).
- [18] S. Jester and H. Falcke, Science with a lunar low-frequency array: From the dark ages of the Universe to nearby exoplanets, *New Astron. Rev.* **53**, 1 (2009).
- [19] N. Aghanim *et al.* (Planck Collaboration), Planck 2018 results. VI. Cosmological parameters, *Astron. Astrophys.* **641**, A6 (2020).
- [20] S. Alexander, E. McDonough, A. Pullen, and B. Shapiro, Physics beyond the standard model with circular polarization in the CMB and CMB-21 cm cross-correlation, *J. Cosmol. Astropart. Phys.* **01** (2020) 032.
- [21] M. A. Alvarez, E. Komatsu, O. Dore, and P. R. Shapiro, The cosmic reionization history as revealed by the

- CMB Doppler-21-cm correlation, *Astrophys. J.* **647**, 840 (2006).
- [22] P. Adshead and S. Furlanetto, Reionization and the large-scale 21 cm-cosmic microwave background cross correlation, *Mon. Not. R. Astron. Soc.* **384**, 291 (2008).
- [23] H. Tashiro, N. Aghanim, M. Langer, M. Douspis, and S. Zaroubi, The cross-correlation of the CMB polarisation and the 21 cm line fluctuations from cosmic reionisation, *Mon. Not. R. Astron. Soc.* **389**, 469 (2008).